

On the Use of Enveloping Distribution Sampling (EDS) to Compute Free Enthalpy Differences between Different Conformational States of Molecules: Application to 3_{10} -, α -, and π -Helices

Zhixiong Lin,^{†,‡} Haiyan Liu,[‡] Sereina Riniker,[†] and Wilfred F. van Gunsteren^{*†}

[†]Laboratory of Physical Chemistry, Swiss Federal Institute of Technology, ETH, 8093 Zürich, Switzerland

[‡]School of Life Sciences and Hefei National Laboratory for Physical Sciences at the Microscale, University of Science and Technology of China (USTC), Hefei, Anhui 230027, People's Republic of China

 Supporting Information

ABSTRACT: Enveloping distribution sampling (EDS) is a powerful method to compute relative free energies from simulation. So far, the EDS method has only been applied to alchemical free energy differences, i.e., between different Hamiltonians defining different systems, and not yet to obtain free energy differences between different conformations or conformational states of a system. In this article, we extend the EDS formalism such that it can be applied to compute free energy differences of different conformations and apply it to compute the relative free enthalpy ΔG of 3_{10} -, α -, and π -helices of an alanine deca-peptide in explicit water solvent. The resulting ΔG values are compared to those obtained by standard thermodynamic integration (TI) and from so-called end-state simulations. A TI simulation requires the definition of a λ -dependent pathway which in the present case is based on hydrogen bonds of the different helical conformations. The values of $\langle (\partial V_{\text{TI}}) / (\partial \lambda) \rangle_{\lambda}$ show a sharp change for a particular range of λ values, which is indicative of an energy barrier along the pathway, which lowers the accuracy of the resulting ΔG value. In contrast, in a two-state EDS simulation, an unphysical reference-state Hamiltonian which connects the parts of conformational space that are relevant to the different end states is constructed automatically; that is, no pathway needs to be defined. In the simulation using this reference state, both helices were sampled, and many transitions between them occurred, thus ensuring the accuracy of the resulting free enthalpy difference. According to the EDS simulations, the free enthalpy differences of the π -helix and the 3_{10} -helix versus the α -helix are 5 kJ mol⁻¹ and 47 kJ mol⁻¹, respectively, for an alanine deca-peptide in explicit SPC water solvent using the GROMOS 53A6 force field. The EDS method, which is a particular form of umbrella sampling, is thus applicable to compute free energy differences between conformational states as well as between systems and has definite advantages over the traditional TI and umbrella sampling methods to compute relative free energies.

1. INTRODUCTION

Calculation of free energy differences is fundamental in order to understand the properties of physical, chemical, and biological systems and phenomena. Consequently, it has for a long time been one of the central tasks of molecular simulation. Molecular dynamics (MD) simulations are widely used for such calculations.^{1–12} The ability to calculate relative free energies from MD simulations not only allows one to understand the underlying processes at the atomic level but also to probe unstable states of a system that are experimentally not accessible. Applications of free energy simulations include processes such as solvation,^{13,14} ligand binding,^{15,16} peptide/protein folding,^{17,18} ion transport,¹⁹ and so on. In order to obtain accurate free energy differences, two main challenges have to be met. First, a model for the system has to be made, i.e., a Hamiltonian or force field, that must correctly describe the thermodynamic behavior of the system. Second, an efficient scheme to calculate relative free energies from a configurational ensemble has to be found. In this article, we will concentrate on the second challenge.

Free energy differences in molecular systems can be classified into two main categories.²⁰ One is the free energy difference between different conformations or conformational states of a molecule. Typical examples include the evaluation of the free

energies of folding, of different helical and hairpin structures,^{21,22} and of transportation of ions over membranes. The other category comprises the alchemical free energy difference between different Hamiltonians, e.g., different molecules or molecular systems. Typical examples include the evaluation of relative free energies of solvation and binding.

There exists a great variety of methods for calculating relative free energies.^{1,2,4,5,8,10–12} The traditional ones for the calculation of relative conformational free energies are direct counting of the different conformations in an unbiased simulation and umbrella sampling²³ using one or more biasing potential energy functions that enhance the sampling of particular conformations. In the counting method, the free energy is calculated directly from the ratio of the numbers of sampled configurations belonging to each state. Thus, it fails if one of the conformational states is insufficiently sampled, i.e., is not stable or if there are high barriers between them. The umbrella sampling method, on the other hand, relies on the choice of a pathway and the use of a biasing potential energy term in the Hamiltonian that forces the sampling going from one state to the other. Some recently

Received: September 5, 2011

Published: October 28, 2011

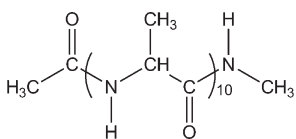


Figure 1. Chemical formula of the alanine deca-peptide studied: acetyl-(Ala)₁₀-N-methyl.

developed and sophisticated methods include local elevation umbrella sampling (LEUS)²⁴ and ball-and-stick LEUS.²⁰

In regard to alchemical perturbations, the established methods are thermodynamic integration²⁵ (TI) and free energy perturbation²⁶ (FEP). The Hamiltonians of the two different states are connected by the introduction of a coupling parameter λ . Thus, a pathway $V(\lambda)$ is defined in order to sample from one state to the other. In the TI method, the quantity $(\partial V)/(\partial \lambda)$ is averaged and integrated along the pathway. In the multistep FEP method, independent simulations at different λ values are performed, and subsequently exponential averaging is used to determine the free energy differences between neighboring λ values, which are added up to give the total free energy difference. The limitations of these two methods are, first, that a significant amount of simulation time is spent on the noninteresting (generally unphysical) intermediate states along the pathway in order to obtain enough overlap of the sampled phase space between the two states of interest. Second, the choice of a pathway $V(\lambda)$ which allows optimal sampling and convergence of the averages for each value of λ is not trivial. Therefore, some methods avoid the definition of a pathway of intermediate states and only rely on sampling of the two end states. For example, one may take the crossing point of the energy difference distributions as an estimation of the free energy difference,^{27,28} or the mean of the FEP results obtained from the two end states in the two directions, or Bennett's acceptance ratio method,^{29,30} or more generalized overlap sampling methods.^{31,32} In these methods, no pathway needs to be defined, but the overlap of the phase spaces relevant to two end states is required. Third, these methods are limited to two-state problems. For this reason, FEP has been generalized to be able to calculate relative free energies of multiple states from a single simulation of a possibly unphysical reference Hamiltonian in the so-called "one-step perturbation" method.^{16,33} Thus, no pathway has to be defined as well. However, one-step perturbation will fail if there is not enough overlap of the sampled phase space of the reference state and that of the end states. This led to the development of the method of enveloping distribution sampling (EDS).^{34–39} In the EDS method, the parameters of an unphysical reference-state Hamiltonian are iteratively optimized such that the different end states are most uniformly sampled in a single simulation, thus ensuring the accuracy of the resulting relative free energies. Using EDS, no pathway of intermediate states, e.g., a $V(\lambda)$, needs to be chosen; it is defined through the general form of the EDS Hamiltonian, which has a functional form that is solely defined by the functional forms of the end-state Hamiltonians in combination with two parameters, the smoothness parameter s_{BA} , and the reference energy offset difference ΔE_{BA}^R per pair of end states A and B, and through the procedure to optimize the s_{BA} and ΔE_{BA}^R parameters. No λ dependence of the Hamiltonian needs to be specified, only end-state Hamiltonians. In principle, EDS can be applied to multiple end-state problems, and to the case where there is no overlap between the end states.³⁵

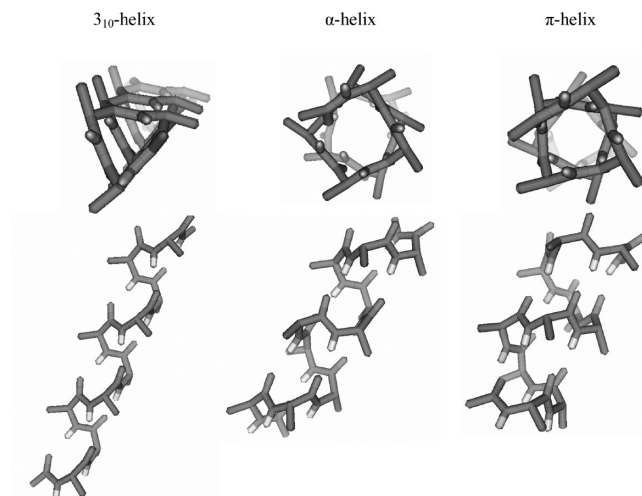


Figure 2. Top and side views of the three helices of the alanine deca-peptide.

So far, the EDS method has only been applied to alchemical free energy differences^{34–39} and not yet been used to obtain the relative free energy of different conformations or conformational states. In this article, we investigate the use of EDS to obtain the free enthalpy differences between different conformations of a solute molecule, i.e., 3_{10} -, α -, and π -helices of an alanine deca-peptide (Figures 1 and 2) in aqueous solution, and compare the results with those obtained by TI using a particular $V(\lambda)$ and by calculations from end-state simulations. We only consider two two-state problems, i.e., the free enthalpy difference between the α - and the π -helix and between the α - and the 3_{10} -helix.

2. THEORY

Assume we wish to calculate the free enthalpy difference between two conformations, α and β , of a molecule, and one or both of them is not the most stable one of the molecule. We may use the EDS technique to obtain the free enthalpy difference by defining the EDS reference Hamiltonian as follows.

Two restraining energy function terms are defined which restrain the molecular conformations to conformation α or to conformation β , i.e., $V_X^{\text{rest}}(\vec{r}^N; K_X^{\text{rest}}, \vec{r}_{0\xi}^N)$ where $X = A$ or B and $\vec{r}_{0\xi}^N$ is the set of parameters which characterizes the conformation ξ , $\xi = \alpha$ or β , e.g., through particular hydrogen-bond distance ranges or torsional-angle ranges, and K_X^{rest} is the restraining force constant. Thus, the resulting Hamiltonian for the end state X is

$$V_X(\vec{r}^N) = V_X^{\text{rest}}(\vec{r}^N; K_X^{\text{rest}}, \vec{r}_{0\xi}^N) + V^{\text{phys}}(\vec{r}^N) \quad (1)$$

where $V^{\text{phys}}(\vec{r}^N)$ is the interaction function of a particular force field. Then, we may construct an EDS reference-state Hamiltonian:

$$\begin{aligned} V_R(\vec{r}^N; s, E_{BA}^R) &= -k_B T s^{-1} \ln \{ e^{-s(V_A^{\text{rest}}(\vec{r}^N) - E_A^R)/k_B T} \\ &\quad + e^{-s(V_B^{\text{rest}}(\vec{r}^N) - E_B^R)/k_B T} \} + V^{\text{phys}}(\vec{r}^N) \\ &= V^{\text{EDS, rest}}(\vec{r}^N; s, E_{BA}^R) + V^{\text{phys}}(\vec{r}^N) \end{aligned} \quad (2)$$

where s is a smoothness parameter and $E_B^R - E_A^R = E_{BA}^R$ is an energy offset parameter difference, which are chosen such as to optimize the sampling of both end states A and B.

In the original EDS implementation, the configurations \vec{r}^N that are sampled by the reference Hamiltonian H_R , i.e., V_R are not assigned to any conformational states. They are considered³⁴ to belong to state A if

$$(V_A^{\text{rest}}(\vec{r}^N) - E_A^R) < (V_B^{\text{rest}}(\vec{r}^N) - E_B^R) \quad (3)$$

In the case considered here, configurations must be separated into different sets, i.e., different conformational states: they belong to set α if

$$V_A^{\text{rest}}(\vec{r}^N) \leq E_{\alpha}^{\text{thres}} \text{ and } V_B^{\text{rest}}(\vec{r}^N) > E_{\beta}^{\text{thres}} \quad (4)$$

they belong to set β if

$$V_A^{\text{rest}}(\vec{r}^N) > E_{\alpha}^{\text{thres}} \text{ and } V_B^{\text{rest}}(\vec{r}^N) \leq E_{\beta}^{\text{thres}} \quad (5)$$

or they may belong to neither of them, called sets γ and δ with set γ defined by

$$V_A^{\text{rest}}(\vec{r}^N) > E_{\alpha}^{\text{thres}} \text{ and } V_B^{\text{rest}}(\vec{r}^N) > E_{\beta}^{\text{thres}} \quad (6)$$

and set δ defined by

$$V_A^{\text{rest}}(\vec{r}^N) \leq E_{\alpha}^{\text{thres}} \text{ and } V_B^{\text{rest}}(\vec{r}^N) \leq E_{\beta}^{\text{thres}} \quad (7)$$

Generally, set δ should contain no or only a few configurations in order to make a meaningful distinction between sets α and β .

Here, the configurations that belong to sets α and β are defined via an energy threshold criterion E_{ξ}^{thres} , which maps configurations \vec{r}^N onto an energy $V_X^{\text{rest}}(\vec{r}^N)$ using the same function $V_X^{\text{rest}}(\vec{r}^N)$ that is used in the reference Hamiltonian. This means that the configurations that belong to sets α and β are defined through eqs 4 and 5, respectively. We note that these sets α and β differ from the conformational ensembles A and B that are through the end-state Hamiltonians defined by eq 1.

Alternatively, the conformational sets α and β could be defined using a geometric measure such as an atom-positional root-mean-square deviation (RMSD) from a given configuration, either in Cartesian or in internal torsional coordinates, instead of using the restraining functions V_X^{rest} and threshold energies E_{ξ}^{thres} . Configurations then belong to set α if

$$\text{RMSD}(\vec{r}^N, \vec{r}_{\alpha}^N) \leq \text{RMSD}_{\alpha}^{\text{thres}} \text{ and } \text{RMSD}(\vec{r}^N, \vec{r}_{\beta}^N) > \text{RMSD}_{\beta}^{\text{thres}} \quad (8)$$

they belong to set β if

$$\text{RMSD}(\vec{r}^N, \vec{r}_{\alpha}^N) > \text{RMSD}_{\alpha}^{\text{thres}} \text{ and } \text{RMSD}(\vec{r}^N, \vec{r}_{\beta}^N) \leq \text{RMSD}_{\beta}^{\text{thres}} \quad (9)$$

or they belong to neither of them, called set γ and set δ :

$$\gamma : \text{RMSD}(\vec{r}^N, \vec{r}_{\alpha}^N) > \text{RMSD}_{\alpha}^{\text{thres}} \text{ and } \text{RMSD}(\vec{r}^N, \vec{r}_{\beta}^N) > \text{RMSD}_{\beta}^{\text{thres}} \quad (10)$$

$$\delta : \text{RMSD}(\vec{r}^N, \vec{r}_{\alpha}^N) \leq \text{RMSD}_{\alpha}^{\text{thres}} \text{ and } \text{RMSD}(\vec{r}^N, \vec{r}_{\beta}^N) \leq \text{RMSD}_{\beta}^{\text{thres}} \quad (11)$$

Again, the thresholds $\text{RMSD}_{\xi}^{\text{thres}}$ should be chosen such that set δ contains no or only a few configurations.

In the procedure and expressions used in the optimization of the parameters s and $E_B^R = E_{BA}^R$ (E_A^R is standardly set to zero in two-state EDS), configurations that belong to sets γ and δ can be ignored. Thus, we get for updating the energy offset

E_B^R (corresponds to eq 13 of ref 36):

$$E_B^R(\text{new}) = -k_B T \ln \left\langle \left\{ e^{-(V_A^{\text{rest}} - V_B^{\text{rest}} + E_B^R(\text{old})) / k_B T} + 1 \right\}^{-1} \right\rangle_{R, \text{not}\gamma, \text{not}\delta} + E_B^R(\text{old}) \quad (12)$$

where configurations of sets γ and δ are excluded when calculating the ensemble average over the ensemble of the reference state R.

For updating or rather choosing a new s parameter, we calculate

$$s_A = -\left\{ \ln \left\langle e^{-(|V_B^{\text{rest}} - V_A^{\text{rest}}| - E_{BA}^R) / k_B T} \right\rangle_A \right\}^{-1} \quad (13)$$

and

$$s_B = -\left\{ \ln \left\langle e^{-(|V_A^{\text{rest}} - V_B^{\text{rest}}| + E_{BA}^R) / k_B T} \right\rangle_B \right\}^{-1} \quad (14)$$

and take the lowest s value as the new s

$$s = \min(s_A, s_B) \quad (15)$$

which corresponds to eq 14 of ref 36.

Ensembles A and B are obtained by reweighting the configurations generated using the reference state R to the corresponding end state A or B. For a quantity $Q(\vec{r}^N)$, which is a function of the coordinates \vec{r}^N , we have

$$\langle Q \rangle_X = \frac{\int Q(\vec{r}^N) e^{-V_X(\vec{r}^N) / k_B T} d\vec{r}^N}{\int e^{-V_X(\vec{r}^N) / k_B T} d\vec{r}^N} \quad (16)$$

or using the ensemble R

$$\langle Q \rangle_X = \frac{\langle Q e^{-(V_X - V_R) / k_B T} \rangle_R}{\langle e^{-(V_X - V_R) / k_B T} \rangle_R} \quad (17)$$

Subsequently, the ensemble averaging in eq 17 could be restricted to the sets α and β . In that case, these restricted ensemble averages can be written as

$$\begin{aligned} \langle Q \rangle_A &= \frac{\langle Q e^{-(V_A - V_R) / k_B T} \rangle_{R, \text{not}\gamma, \text{not}\delta}}{\langle e^{-(V_A - V_R) / k_B T} \rangle_{R, \text{not}\gamma, \text{not}\delta}} \\ &= \frac{\langle Q e^{-[V_A^{\text{rest}} - V^{\text{EDS, rest}}(s, E_{BA}^R)] / k_B T} \rangle_{R, \text{not}\gamma, \text{not}\delta}}{\langle e^{-[V_A^{\text{rest}} - V^{\text{EDS, rest}}(s, E_{BA}^R)] / k_B T} \rangle_{R, \text{not}\gamma, \text{not}\delta}} \end{aligned} \quad (18)$$

and

$$\begin{aligned} \langle Q \rangle_B &= \frac{\langle Q e^{-(V_B - V_R) / k_B T} \rangle_{R, \text{not}\gamma, \text{not}\delta}}{\langle e^{-(V_B - V_R) / k_B T} \rangle_{R, \text{not}\gamma, \text{not}\delta}} \\ &= \frac{\langle Q e^{-[V_B^{\text{rest}} - V^{\text{EDS, rest}}(s, E_{BA}^R)] / k_B T} \rangle_{R, \text{not}\gamma, \text{not}\delta}}{\langle e^{-[V_B^{\text{rest}} - V^{\text{EDS, rest}}(s, E_{BA}^R)] / k_B T} \rangle_{R, \text{not}\gamma, \text{not}\delta}} \end{aligned} \quad (19)$$

In this way, erratic irrelevant energy values due to irrelevant configurations not belonging to sets α and β are excluded from influencing the parameter optimization for sampling of sets α and β . Furthermore, configurations which belong to set δ that have low V_X^{rest} values are excluded too.

Table 1. Overview of the Simulations

end-state simulations					
simulations	initial structure	simulation time [ns]	no. of solvent molecules	$\langle V_x^{\text{rest}} \rangle [\text{kJ mol}^{-1}]$	av. hydrogen bonds [%]
3 ₁₀ -helix	3 ₁₀ -helix	11	4336	31.7	65
α -helix	α -helix	11	3204	3.7	59
π -helix	π -helix	11	2660	1.9	71
thermodynamic integration (TI) simulations					
simulations	initial structure	simulation time [ns]	no. of solvent molecules		
α -helix \rightarrow π -helix	α -helix	11 \times 2	3204		
α -helix/ π -helix EDS parameter update simulations					
simulations	initial structure	simulation time [ns]	no. of solvent molecules	update scheme	
update1	α -helix	128 \times 0.15	3204	update after 1, 3, 7, 13... of 0.15 ns simulations	
update2	π -helix	128 \times 0.15	2660	update after 1, 3, 7, 13... of 0.15 ns simulations	
update3	α -helix	128 \times 0.15	3204	update after 1, 3, 7, 15... of 0.15 ns simulations	
update4	π -helix	128 \times 0.15	2660	update after 1, 3, 7, 15... of 0.15 ns simulations	
update5	α -helix	128 \times 0.15	3204	update after 1, 3, 7, 15... of 0.15 ns simulations, with excluding noninteresting states	
update6	π -helix	128 \times 0.15	2660	update after 1, 3, 7, 15... of 0.15 ns simulations, with excluding noninteresting states	
α -helix/ π -helix EDS evaluation simulations					
simulations	initial structure	simulation time [ns]	no. of solvent molecules	parameters taken from	
EDS1	π -helix	51	2660	update1: $s = 0.16, E_B^R = 13.9$	
EDS2	π -helix	51	2660	update2: $s = 0.21, E_B^R = 10.1$	
EDS3	π -helix	51	2660	update3: $s = 0.30, E_B^R = 7.2$	
EDS5	π -helix	51	2660	update5: $s = 0.16, E_B^R = 14.1$	
α -helix/3 ₁₀ -helix EDS parameter update simulations					
simulations	initial structure	simulation time [ns]	no. of solvent molecules	update scheme	
update7	α -helix	128 \times 0.15	3204	update after 1, 3, 7, 15... of 0.15 ns simulations	
update8	3 ₁₀ -helix	128 \times 0.15	4336	update after 1, 3, 7, 15... of 0.15 ns simulations	
α -helix/3 ₁₀ -helix EDS evaluation simulations					
simulations	initial structure	simulation time [ns]	no. of solvent molecules	parameters taken from	
EDS7	α -helix	51	3204	update7: $s = 0.03, E_B^R = 68.7$	

The free enthalpy difference between two end-state Hamiltonians B and A in the EDS simulation is evaluated through³⁶

$$\Delta G_{BA} = G_B - G_A = \Delta G_{BR} - \Delta G_{AR} = -k_B T \ln \frac{\langle e^{-(H_B - H_R)/k_B T} \rangle_R}{\langle e^{-(H_A - H_R)/k_B T} \rangle_R} \quad (20)$$

The expression used to obtain the free enthalpy difference between conformational sets β and α from an ensemble generated using the reference-state Hamiltonian $V_R(\vec{r}^N; s, E_{BA}^R)$ reads

$$\Delta G_{\beta\alpha} = G_\beta - G_\alpha = -k_B T \ln \left\{ \frac{N_\beta(V^{\text{phys}})}{N_\alpha(V^{\text{phys}})} \right\} \quad (21)$$

where $N_\xi(V^{\text{phys}})$ is the number of configurations belonging to set ξ in an ensemble generated using V^{phys} . In terms of the ensemble R generated using the reference-state potential energy V_R , we get

(see Appendix)

$$\Delta G_{\beta\alpha} = -k_B T \ln \left\{ \frac{\langle e^{+V^{\text{EDS,rest}}/k_B T} \rangle_{R,\text{set}\beta}}{\langle e^{+V^{\text{EDS,rest}}/k_B T} \rangle_{R,\text{set}\alpha}} \times \frac{N_\beta(V_R)}{N_\alpha(V_R)} \right\} \quad (22)$$

In other words, the ensemble R that was generated using the biasing potential energy function $V^{\text{EDS,rest}}$ is reweighted using eq 22, and the configurations of the sets α and β are used in the averaging via their relative populations in the ensemble R , i.e., $N_\alpha(V_R)$ and $N_\beta(V_R)$

$$\frac{N_\beta(V_R)}{N_\alpha(V_R)} = \frac{\langle \delta(\vec{r}^N - \vec{r}_\beta^N) \rangle_R}{\langle \delta(\vec{r}^N - \vec{r}_\alpha^N) \rangle_R} \quad (23)$$

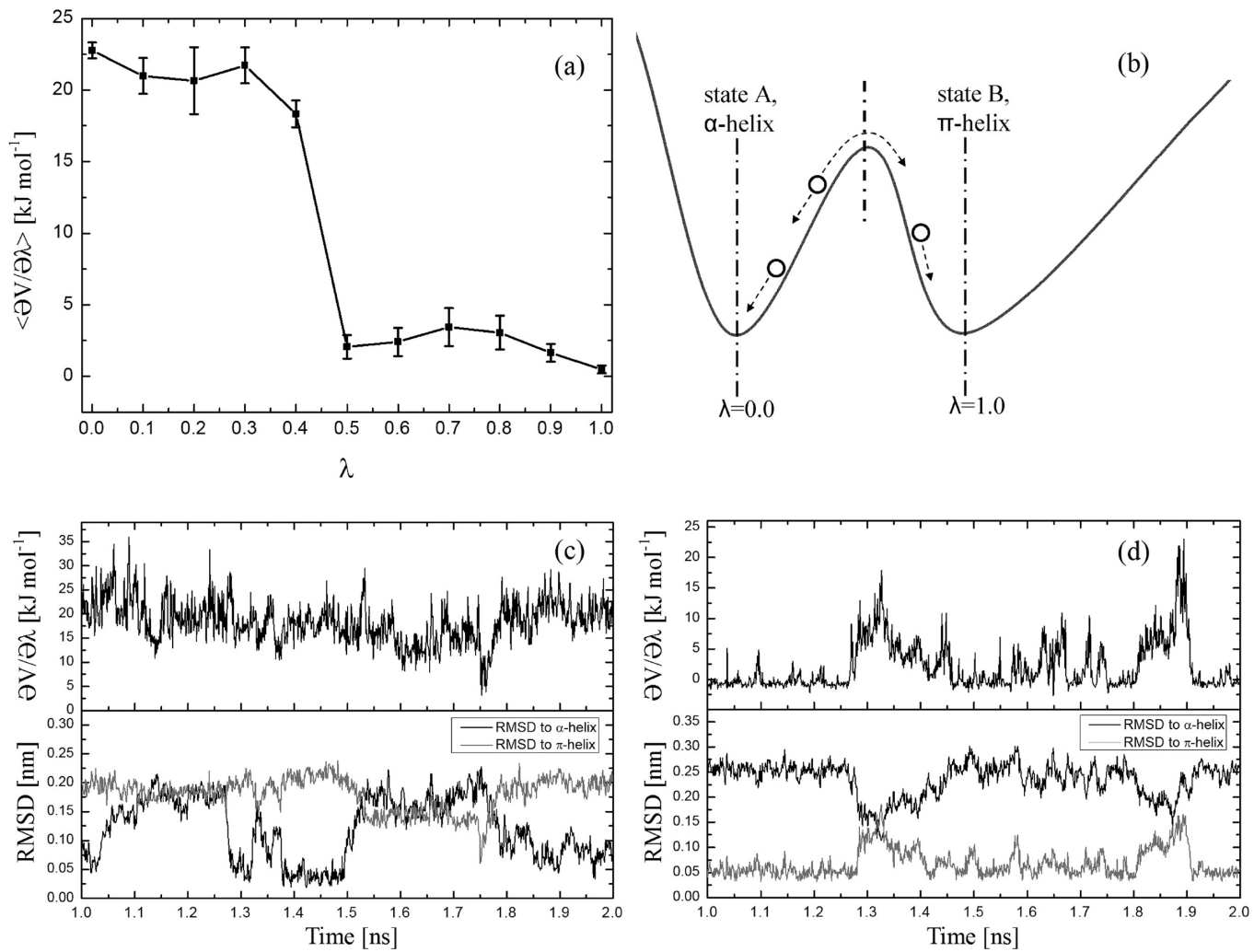


Figure 3. Thermodynamic integration (TI) simulations from state A (α -helix, $\lambda = 0.0$) to state B (π -helix, $\lambda = 1.0$) which restrain alanine deca-peptide into conformational sets α (α -helix) and β (π -helix), respectively. (a) $\langle (\partial V_{\text{TI}}) / (\partial \lambda) \rangle_\lambda$ as a function of λ . (b) A schematic representation of V^{phys} , the nonbiased potential energy at different configurations corresponding to different λ values, and the λ -dependent pathway and real energy barrier between the two states. (c, d) Time evolution of $(\partial V_{\text{TI}}) / (\partial \lambda)$ and backbone atom-positional RMSD of the peptide with respect to the α -helix or the π -helix of the TI simulations at $\lambda = 0.4$ (c) or $\lambda = 0.5$ (d).

Equation 22 can be simply rewritten as

$$\Delta G_{\beta\alpha} = -k_B T \ln \frac{N_\beta(V_R)}{N_\alpha(V_R)} - k_B T \ln \left\langle e^{+V^{\text{EDS, rest}}/k_B T} \right\rangle_{R, \text{set}\beta} + k_B T \ln \left\langle e^{+V^{\text{EDS, rest}}/k_B T} \right\rangle_{R, \text{set}\alpha} \quad (24)$$

Equation 24 is equivalent to the expression used in conformational state-specific one-step perturbation.⁴⁰ In other words, the EDS reference-state Hamiltonian can be used as the reference state in one-step perturbation, ensuring sufficient sampling of the conformational end states, which is reached by optimizing the parameters s and E_{BA}^R .

If simulations based on the end state potential energy functions $V_X(\vec{r}^N)$, see eq 1, are available, these ensembles $X = A$ and $X = B$ can also be used to obtain the free enthalpy difference

between conformational sets β and α (see Appendix):

$$\Delta G_{\beta\alpha} = -k_B T \ln \left\{ \frac{\left\langle e^{+V_B^{\text{rest}}/k_B T} \right\rangle_{B, \text{set}\beta}}{\left\langle e^{+V_A^{\text{rest}}/k_B T} \right\rangle_{A, \text{set}\alpha}} \times \frac{\langle 1 \rangle_{B, \text{set}\beta}}{\langle 1 \rangle_{A, \text{set}\alpha}} \times \frac{\left\langle e^{-(V_M - V_A)/k_B T} \right\rangle_A}{\left\langle e^{-(V_M - V_B)/k_B T} \right\rangle_B} \right\} \quad (25)$$

in which V_M is an intermediate state connecting two end states. If we use the EDS reference-state Hamiltonian as the intermediate state, the ensemble averages in the last factor of eq 25 can be written as

$$\left\langle e^{-(V_M - V_X)/k_B T} \right\rangle_X = \left\langle e^{-(V^{\text{EDS, rest}}(s, E_{BA}^R) - V_X^{\text{rest}})/k_B T} \right\rangle_X \quad (26)$$

We refer to the Appendix for the derivations of eqs 22 and 25.

3. MOLECULAR MODEL AND COMPUTATIONAL METHOD

3.1. Molecular Model, Definition of End-State Hamiltonians, and Conformational Sets. The model system considered is an

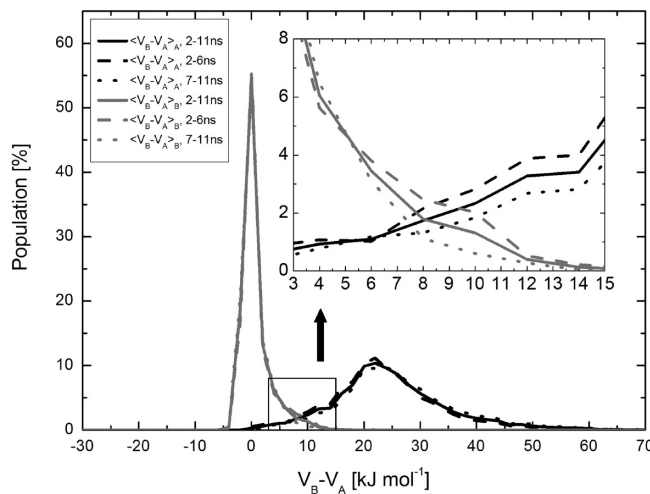


Figure 4. Distributions of the energy difference $V_B - V_A$ in the simulations of end states A (α -helix) and B (π -helix) for different simulation periods.

alanine deca-peptide capped at both termini with methyl groups, acetyl-(Ala)₁₀-N-methyl (Figure 1), solvated in water. The GROMOS force field 53A6⁴¹ was used for the peptide, and the water solvent molecules were represented by a rigid three-site simple-point-charge (SPC)⁴² model.

The restraining potential energy term $V_X^{\text{rest}}(\vec{r}^N; K_X^{\text{rest}}, \vec{r}_{0\xi}^N)$ used to characterize different end-state Hamiltonians is defined as an attractive half-harmonic function applied to all of the hydrogen-bonding pairs of O and H atoms:

$$V_X^{\text{rest}}(\vec{r}^N; K_X^{\text{rest}}, \vec{r}_{0\xi}^N) = \frac{1}{2} K_X^{\text{rest}} \sum_{i=1}^{N_{HB,\xi}} (d_{iX} - d_{0\xi})^2 \text{ when } d_{iX} > d_{0\xi} \\ = 0 \text{ when } d_{iX} \leq d_{0\xi} \quad (27)$$

where $X = A, B$, and C , which restrains the peptide into an α , π , and 3_{10} -helix, respectively (Figure 2). $N_{HB,\xi}$ is the number of hydrogen bonds (8, 7, or 9) of these three helices, and d_{iX} is the distance between the hydrogen bonding O and H atoms (Tables S1–S3, Supporting Information). K_X^{rest} is the force constant, and $d_{0\xi}$ is the reference distance. They were set to 30 kJ mol⁻¹ nm⁻² and 0.25 nm for state A , 150 kJ mol⁻¹ nm⁻² and 0.25 nm for state B , and 2700 kJ mol⁻¹ nm⁻² and 0.19 nm for state C . The parameters were chosen such that in the end-state simulations, the averages of corresponding helical hydrogen-bond populations are about 60–70% (Table 1 and Supporting Information Tables S1–S3 and Figures S1–S3).

The conformational sets α and β corresponding to the helices were defined through atom-positional root-mean-square deviation (RMSD) of the backbone atoms (N, CA, C) of the peptide (including the two termini) from the ideal helix, according to eqs 8 and 9. The three ideal helices (\vec{r}_ξ^N) were defined through the φ and ψ backbone torsional-angle values ($-57.8^\circ, -47.0^\circ$) for the α -helix, ($-57.0^\circ, -70.0^\circ$) for the π -helix, and ($-49.0^\circ, -27.0^\circ$) for the 3_{10} -helix. The RMSD threshold value $\text{RMSD}_\xi^{\text{thres}}$ was set to 0.15 nm for all three helices.

In the TI and EDS simulations, the peptide was solvated in different numbers of water molecules (Table 1). In the end-state simulations, different numbers of solvent molecules were used too, depending on the size of the solute; a minimum distance of 1.4 nm of any solute atom to the walls of the periodic box was required. A test simulation of the π -helix solvated in 3204

Table 2. Free Enthalpy Differences (in kJ mol⁻¹) of the Two End-State Hamiltonians B (π -helix) and A (α -helix), ΔG_{BA} , and the Two Conformational Sets β (π -helix) and α (α -helix), $\Delta G_{\pi\alpha}$ of the Alanine Deca-Peptide in Aqueous Solution^a

	ΔG_{BA}	$\Delta G_{\pi\alpha}$
TI	10.6 ± 1.1	
crossing point	8.1 ± 2	
M1		3.0 ± 0.9
M2		4.1 ± 1.0
M3		4.7 ± 1.2
M4		5.3 ± 1.3
EDS ^c		
EDS1	13.7 ± 0.9	5.6 ± 0.8
EDS2	10.8 ± 0.6	4.5 ± 0.7
EDS3	13.0 ± 0.8	4.5 ± 0.8
EDS5	10.5 ± 0.6	5.6 ± 0.7

^a Statistical uncertainties (except the one for the crossing point) were estimated by block averaging.⁴⁹ ^b End-state simulations: ΔG_{BA} was calculated through the crossing point of the energy difference distributions, see also Figure 2. $\Delta G_{\pi\alpha}$ was calculated through eq 25 using EDS reference-state Hamiltonians as intermediate states. M1: $s = 0.30$, $E_B^R = 7.2$ kJ mol⁻¹. M2: $s = 0.18$, $E_B^R = 12.0$ kJ mol⁻¹. M3: $s = -0.30$, $E_B^R = 0.0$ kJ mol⁻¹. M4: $s = -1.00$, $E_B^R = 0.0$ kJ mol⁻¹. ^c EDS: ΔG_{BA} was calculated through eq 20. $\Delta G_{\pi\alpha}$ was calculated through eq 22. The EDS parameters are given in Table 1.

water molecules did not yield significantly different results (data not shown).

3.2. Thermodynamic Integration (TI). The TI simulations were carried out from state A to state B , which restrain the peptide into the conformational sets α (α -helix) and β (π -helix), respectively. The λ -dependent potential energy term $V(\lambda)$ of the Hamiltonian for the TI simulations was defined as the sum of two attractive half-harmonic functions for the end-state Hamiltonians A and B (eq 27), multiplied by $(1 - \lambda)$ and λ , respectively, added to $V^{\text{phys}}(\vec{r}^N)$:

$$V_{\text{TI}}(\vec{r}^N; \lambda) = (1 - \lambda) \frac{1}{2} K_A^{\text{rest}} \sum_{i=1}^{N_{HB,\alpha}} (d_{ia} - d_{0\alpha})^2 \\ + \lambda \frac{1}{2} K_B^{\text{rest}} \sum_{i=1}^{N_{HB,\beta}} (d_{i\beta} - d_{0\beta})^2 + V^{\text{phys}}(\vec{r}^N) \quad (28)$$

where d_{ia} and $d_{i\beta}$ are the distances between the α -helical or π -helical hydrogen bonding atoms O and H, respectively, and the harmonic restraints are only applied when $d_{i\xi} > d_{0\xi}$. The free enthalpy difference between the two end-state Hamiltonians B and A can be calculated through

$$\Delta G_{BA} = \int_0^1 \left\langle \frac{\partial V_{\text{TI}}}{\partial \lambda} \right\rangle_\lambda d\lambda \quad (29)$$

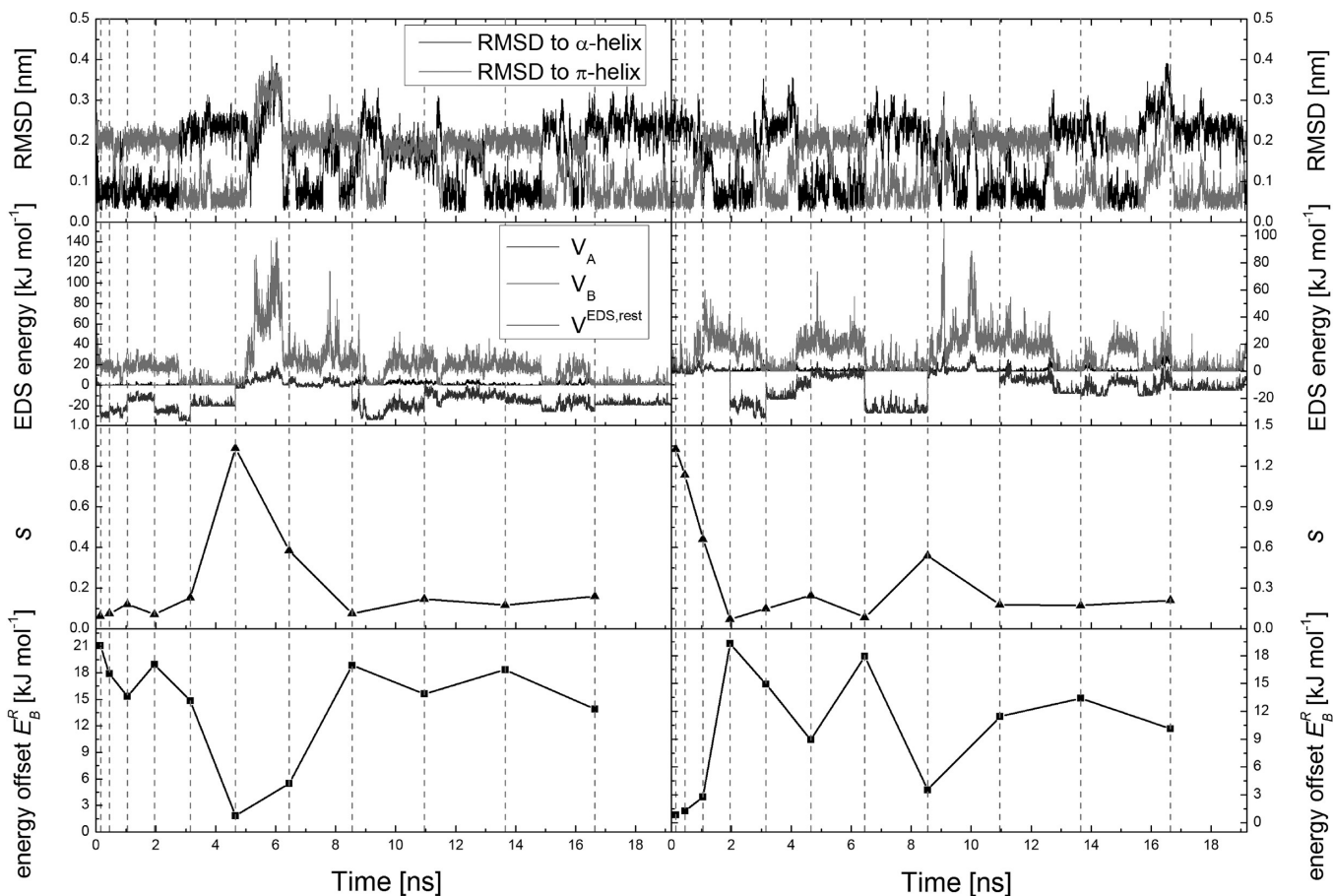


Figure 5. Time evolutions of different properties in the α -helix/ π -helix EDS parameter update simulations *update1* (left panels) and *update2* (right panels), see also Table 1. From top to bottom: backbone atom-positional RMSD of the peptide with respect to the α -helix or π -helix, the restraining and the EDS reference potential energies, smoothness parameter s , energy offset E_B^R . The vertical dashed lines show when the updates of s and E_B^R are carried out.

with

$$\frac{\partial V_{TI}}{\partial \lambda} = -\frac{1}{2} K_A^{\text{rest}} \sum_{i=1}^{N_{HB,\alpha}} (d_{i\alpha} - d_{0\alpha})^2 + \frac{1}{2} K_B^{\text{rest}} \sum_{i=1}^{N_{HB,\beta}} (d_{i\beta} - d_{0\beta})^2$$

when $d_{i\xi} > d_{0\xi}$

$$= 0 \text{ when } d_{i\xi} \leq d_{0\xi} \quad (30)$$

At each of the 11 equidistant λ values, the system was equilibrated for 1 ns followed by 1 ns of production. The final configuration after 1 ns simulation at a λ value was used as the starting configuration for the next λ value.

3.3. End-State Simulations. The three end-state simulations for the three helices were carried out for 11 ns. The energy difference $V_B(\vec{r}^N) - V_A(\vec{r}^N)$ defined through eqs 1 and 27 was calculated in the simulations of the end states A and B. The crossing point of the two distributions of $V_B(\vec{r}^N) - V_A(\vec{r}^N)$ generated in the two simulations was used as an estimate for the free enthalpy difference between the end states B and A. The first 1 ns of both simulations was treated as equilibration time, and the last 10 ns were used to calculate the free enthalpy difference. In addition, the last 10 ns were divided into two continuous 5 ns periods, for which the corresponding distributions and crossing points were also calculated.

The free enthalpy difference between the conformational sets β (π -helix) and α (α -helix) was calculated through eq 25 using four different EDS reference-state Hamiltonians as the intermediate states. M1: $s = 0.30$, $E_{BA}^R = 7.2 \text{ kJ mol}^{-1}$. M2: $s = 0.18$, $E_{BA}^R = 12.0 \text{ kJ mol}^{-1}$. M3: $s = -0.30$, $E_{BA}^R = 0.0 \text{ kJ mol}^{-1}$. M4: $s = -1.00$, $E_{BA}^R = 0.0 \text{ kJ mol}^{-1}$.

3.4. Enveloping Distribution Sampling (EDS) Simulations. Six EDS parameter update simulations were performed to find the optimal reference state parameters for calculating the free enthalpy difference between the π -helix and the α -helix for $128 \times 0.15 \text{ ns}$ (Table 1). Either the α -helix or the π -helix served as the initial configuration. The parameters s and $E_B^R = E_{BA}^R$ (E_A^R is standardly set to zero in two-state EDS) were updated at fixed time points: after the first, third, seventh, and 13th etc. 0.15 ns simulation periods, or after the first, third, seventh, and 15th etc. 0.15 ns simulation periods. That is, the simulation time period was either increased by 0.3 ns or doubled after each update. The new s and E_B^R parameters were calculated without excluding any configurations or with excluding the noninteresting conformational sets γ and δ through eqs 12, 18, and 19. We refer to ref 36 for details of the updating scheme.

Four of the six resulting s and E_B^R parameters were used for EDS evaluation simulations of 51 ns (Table 1). The free enthalpy difference between the two end states, i.e. ΔG_{BA} , was calculated through eq 20, and the free enthalpy difference between the two conformational sets, i.e. $\Delta G_{\pi\alpha}$, was calculated through eq 22.

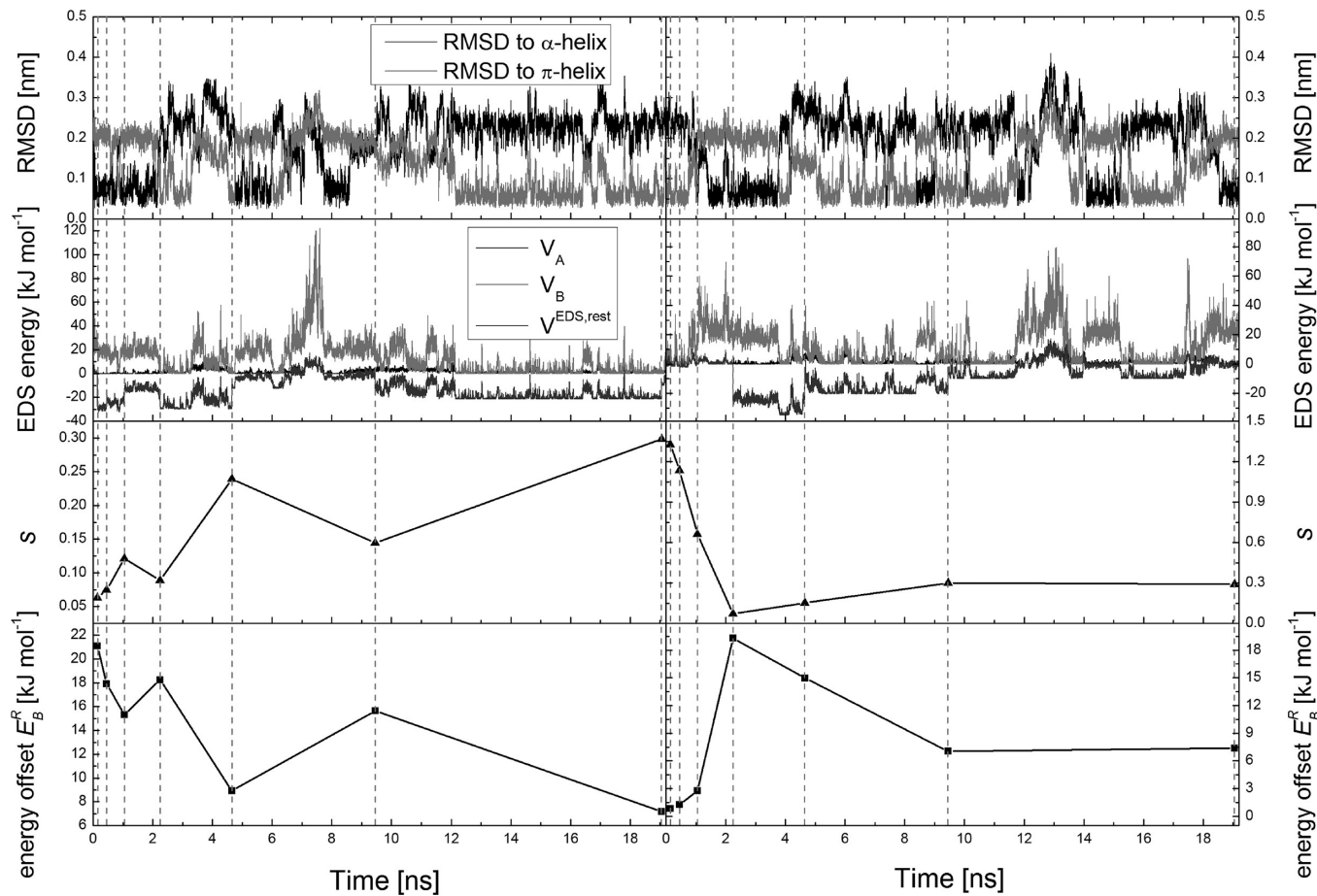


Figure 6. Time evolutions of different properties in the α -helix/ π -helix EDS parameter update simulations *update3* (left panels) and *update4* (right panels), see also Table 1. From top to bottom: backbone atom-positional RMSD of the peptide with respect to the α -helix or π -helix, the restraining and the EDS reference potential energies, smoothness parameter s , energy offset E_B^R . The vertical dashed lines show when the updates of s and E_B^R are carried out.

Two EDS parameter update simulations and one EDS evaluation simulation was carried out for calculating the free enthalpy difference between the 3_{10} -helix and the α -helix (Table 1).

3.5. Simulation Setup and Analysis. The starting configurations of the α -, π -, and 3_{10} -helices were constructed by setting all of the φ and ψ backbone torsional angles to $(-57.8^\circ, -47.0^\circ)$, $(-57.0^\circ, -70.0^\circ)$, and $(-49.0^\circ, -27.0^\circ)$, respectively. The initial configurations were first energy-minimized in a vacuum with all hydrogen bonds restrained. Each of them was then solvated in a rectangular box containing explicit SPC⁴² water. The resulting numbers of water molecules are listed in Table 1. The solvated configurations were further energy minimized to remove possible steric clashes. These configurations were used as the reference configurations for the atom-positional RMSD calculations. An equilibration scheme was carried out for each system. The atom velocities were generated from a Maxwell distribution at 60 K, and the simulation temperature was gradually raised to 300 K, while the strength of the position-restraining potential energy term for the solute atoms was decreased from 2.5×10^4 kJ mol⁻¹ nm⁻² to 25 kJ mol⁻¹ nm⁻².

The simulations were carried out at a constant temperature of 300 K and a constant pressure of 1 atm using the GROMOS simulation package.^{43–45} The solute molecules and the water solvent were separately coupled to a temperature bath at 300 K

by means of weak coupling,⁴⁶ using a relaxation time of 0.1 ps. The pressure was calculated with a molecular virial and held constant by weak coupling⁴⁶ to an external pressure bath with a relaxation time of 0.5 ps, using an isothermal compressibility of 4.575×10^{-4} (kJ mol⁻¹ nm⁻³)⁻¹. All bond lengths and the geometry of the water molecules were constrained using the SHAKE algorithm⁴⁷ with a relative geometric accuracy of 10^{-4} , allowing a time step of 2 fs in the leapfrog algorithm to integrate the equations of motion. For the treatment of the nonbonded interactions, twin-range cutoff radii of 0.8/1.4 nm were used. Interactions within 0.8 nm were evaluated every time step. The intermediate range interactions were updated every fifth time step, and the long-range electrostatic interactions beyond 1.4 nm were approximated by a reaction field force⁴⁸ according to a dielectric continuum with a dielectric permittivity of 61.

Trajectory coordinates and energies were stored at 1 ps intervals for analysis. Atom-positional RMSDs were calculated after translational superposition of solute centers of mass and rotational least-squares fitting of the atomic coordinates of all backbone atoms of the alanine deca-peptide. Hydrogen bonds were defined by a maximum H-atom-acceptor distance of 0.25 nm and a minimum donor-H atom-acceptor angle of 135°.

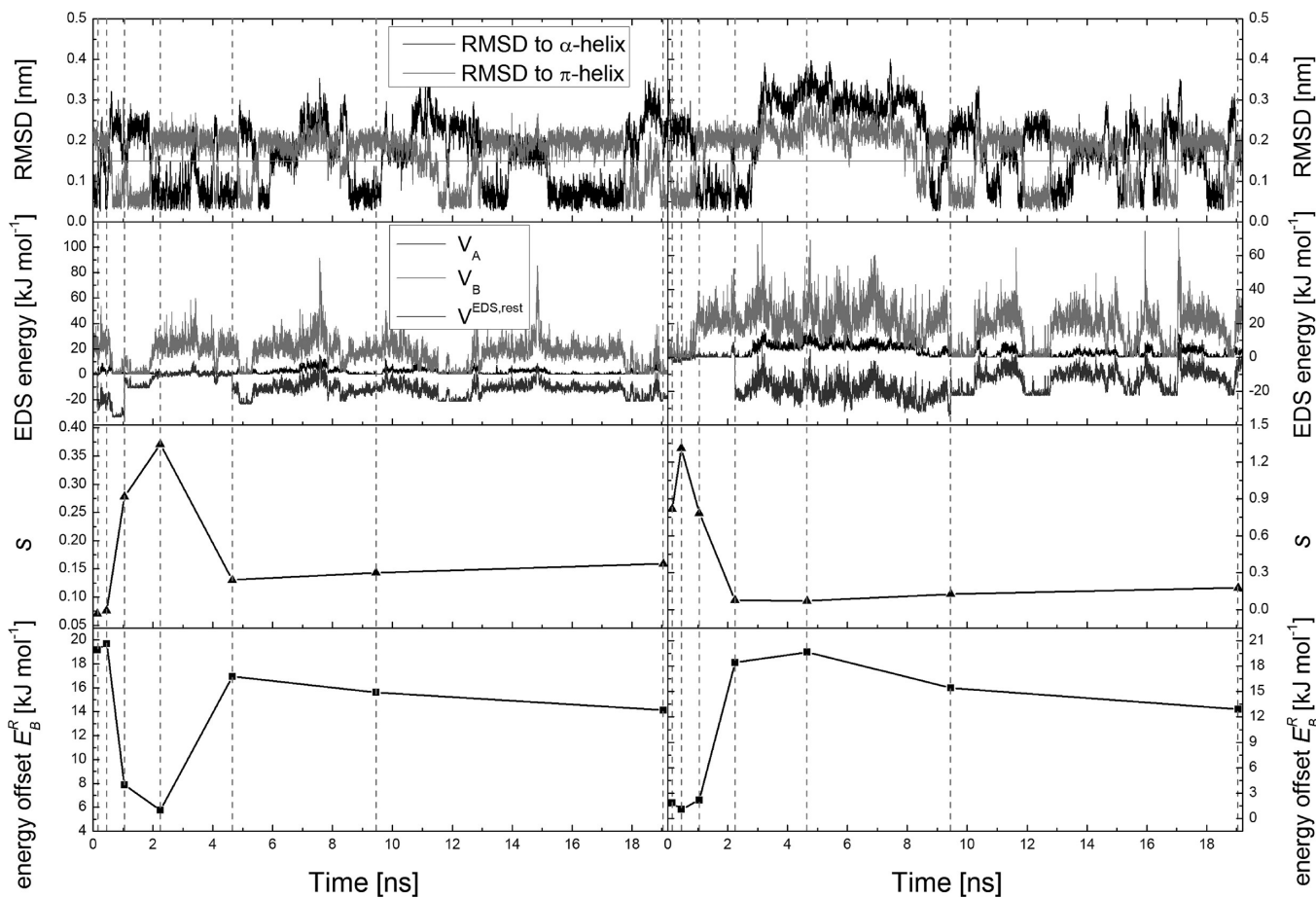


Figure 7. Time evolutions of different properties in the α -helix/ π -helix EDS parameter update simulations *update5* (left panels) and *update6* (right panels), see also Table 1. From top to bottom: backbone atom-positional RMSD of the peptide with respect to the α -helix or π -helix, the restraining and the EDS reference potential energies, smoothness parameter s , energy offset E_B^R . The horizontal gray line represents an RMSD of 0.15 nm used to define set α (α -helix) and set β (π -helix); the vertical dashed lines show when the updates of s and E_B^R are carried out.

4. RESULTS AND DISCUSSION

4.1. Free Enthalpy Estimation from Thermodynamic Integration (TI) Simulations. $\langle (\partial V_{\text{TI}})/(\partial \lambda) \rangle_\lambda$ as a function of λ in the TI simulations is shown in Figure 3a. This curve presents two unusual features. First, there is a sudden change of $\langle (\partial V_{\text{TI}})/(\partial \lambda) \rangle_\lambda$ between λ values 0.4 and 0.5. Second, the first five λ values have a similar value for $\langle (\partial V_{\text{TI}})/(\partial \lambda) \rangle_\lambda$, and the last six λ values have again a similar value. The backbone atom-positional RMSD of the peptide in the simulations at λ values 0.4 and 0.5 are shown in Figure 3c and d together with $\langle (\partial V_{\text{TI}})/(\partial \lambda) \rangle_\lambda$. When $\lambda = 0.4$, the α -helical conformation was mostly sampled, whereas at $\lambda = 0.5$ mainly the π -helical conformation was sampled. This can explain the sharp drop in the $\langle (\partial V_{\text{TI}})/(\partial \lambda) \rangle_\lambda$ curve. Some attempts of transition between the two helices also occurred during the simulations.

If we look closer at the λ -dependent pathway between the two end states of the TI simulation, as shown by a schematic representation of V^{phys} in Figure 3b, state A and state B , which restrain the peptide into the α -helix and the π -helix, respectively, are in different local minima. There is a barrier between them, and the pathway defined by eq 28 crosses the barrier. Thus, at small λ values, the system remained in the local minimum of state A , and mostly the α -helix was sampled. At large λ values, on the other hand, the system stayed in state B , and mostly the π -helix

was sampled. At the intermediate λ values, transitions between two helices should occur but are rare, which affects the convergence of $\langle (\partial V_{\text{TI}})/(\partial \lambda) \rangle_\lambda$. Since the barrier hinders an accurate evaluation of $\langle (\partial V_{\text{TI}})/(\partial \lambda) \rangle_\lambda$ at these λ values, the integral in eq 25 is not very precise.

The free enthalpy difference between two end states B and A , i.e., ΔG_{BA} , obtained by TI using eq 29 is $10.6 \pm 1.1 \text{ kJ mol}^{-1}$. In view of the discussion above, the statistical uncertainty estimated by block averaging⁴⁹ underestimates the real error bar. To calculate the free enthalpy difference between the two conformational sets β (π -helix) and α (α -helix), i.e. $\Delta G_{\pi\alpha}$ reweighting must be applied.

4.2. Free Enthalpy Estimation from End-State Simulations. The distributions of $V_B - V_A$ in the simulations of both end states are shown in Figure 4, in which the crossing point can be used as an estimate for the free enthalpy difference between the two end states B and A , i.e. ΔG_{BA} . The result obtained is 8.1 kJ mol^{-1} . The energy distributions of the first 5 ns and second 5 ns of the simulations differ in the tail parts (inset of Figure 4), which means that the result suffers from statistical uncertainty. In fact, the crossing points of distributions averaged over different simulation periods range from less than 7 kJ mol^{-1} to more than 10 kJ mol^{-1} , indicating that the statistical uncertainty of the result is about 2 kJ mol^{-1} .

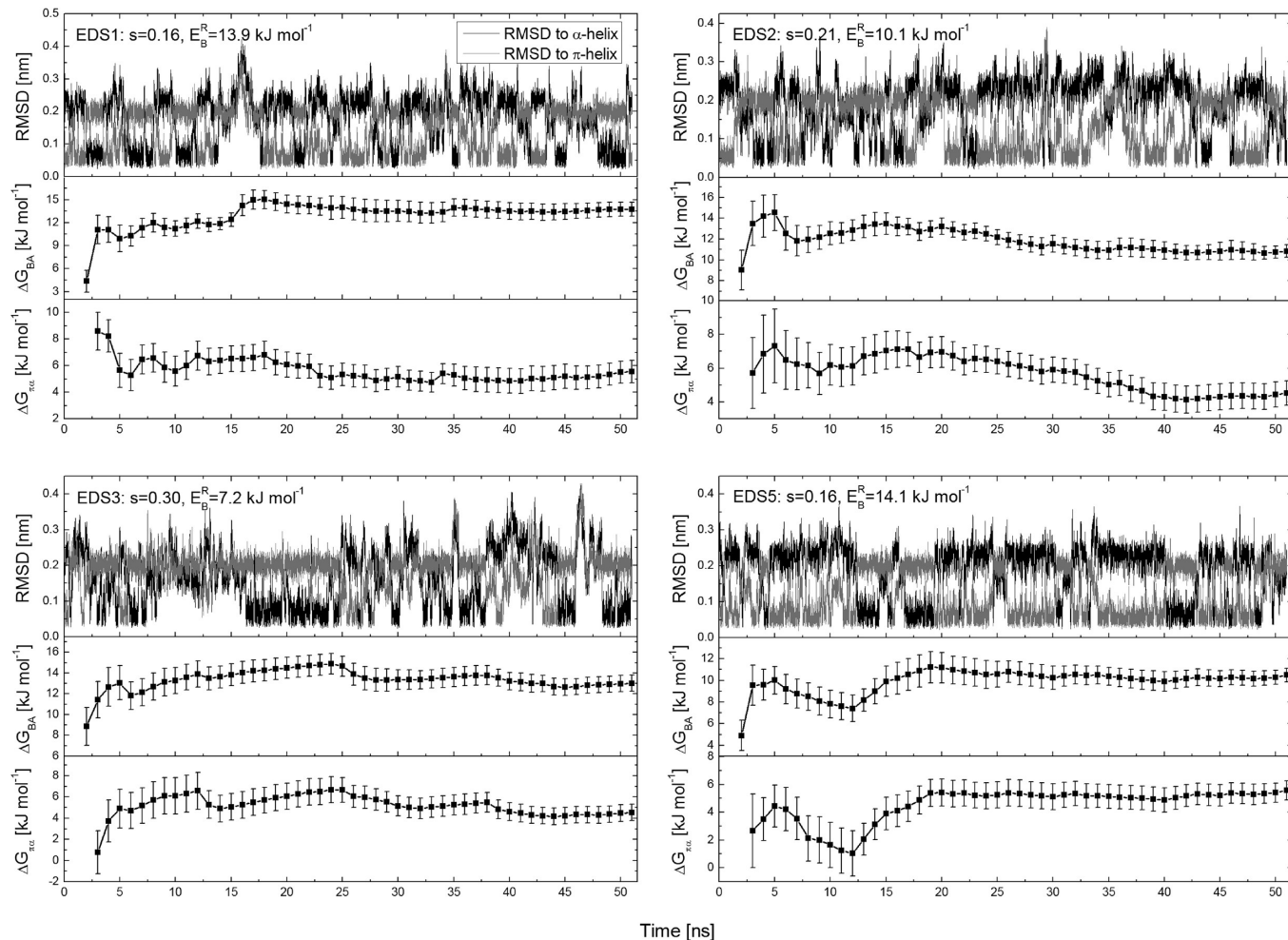


Figure 8. Time evolutions of backbone atom-positional RMSD of the peptide with respect to the α -helix or π -helix, free enthalpy differences of the two end-state Hamiltonians B (π -helix) and A (α -helix), ΔG_{BA} , and free enthalpy differences of the two conformational sets β (π -helix) and α (α -helix), $\Delta G_{\pi\alpha}$, in four EDS evaluation simulations.

The free enthalpy differences between the two conformational sets β (π -helix) and α (α -helix) calculated through eq 25 are listed in Table 2 for the four different EDS reference-state Hamiltonians used as intermediate states, of which two have positive s parameters and the other two have negative s parameters. $s > 0$ corresponds to an EDS reference-state Hamiltonian which envelopes the parts of configuration space of both states A and B, while $s < 0$ results in an EDS reference-state Hamiltonian which is a subset of both states A and B.³⁵ The results of EDS reference-state Hamiltonians with the negative s parameters as the intermediate states should be more reliable, because $\langle e^{-(V_M - V_A)/k_B T} \rangle_A$ and $\langle e^{-(V_M - V_B)/k_B T} \rangle_B$ in eq 25 are more accurate if V_M is sampling a subset of the conformations belonging to V_A and V_B , assuming that the two end states have overlapping conformational spaces, and that these are sufficiently sampled. This method is in principle very similar to the overlap sampling method,^{31,32} the only difference being the choice of the intermediate state. Thus, the overlap sampling method can also be generalized to the free energy calculation of different conformational states.

4.3. Free Enthalpy Estimation from Enveloping Distribution Sampling (EDS) Simulations. The backbone atom-positional RMSD of the peptide for the EDS parameter update

simulations *update1* and *update2* are shown in the upper panels of Figure 5. Both α - and π -helices were sampled during the simulations; the typical residence time between transitions was on the time scale of nanoseconds. The smoothness parameter s and the energy offset parameter E_B^R show strong anticorrelations during the update procedure (bottom panels of Figure 5). The evolution of the parameters is highly dependent on the configurations sampled; therefore they show large fluctuations during the update procedure. The same quantities for the EDS parameter update simulations with increasing simulation time periods between updates, *update3* and *update4*, are shown in Figure 6. Longer time periods ensured more transitions between the two helical conformations, thus reducing the fluctuations of the parameters to a certain extent. The exclusion of the less relevant conformations, sets γ and δ , during the update procedure did not influence the fluctuations and therefore did not improve the convergence of the parameters (Figure 7).

The resulting values for the s and E_B^R parameters are 0.16 and 13.9 kJ mol^{-1} , 0.21 and 10.1 kJ mol^{-1} , 0.30 and 7.2 kJ mol^{-1} , 0.29 and 7.4 kJ mol^{-1} , 0.16 and 14.1 kJ mol^{-1} , and 0.18 and 12.9 kJ mol^{-1} for the six update simulations, respectively. It seems to be difficult to reach convergence to unique optimal parameters, but all of the resulting s and E_B^R parameter values are in a

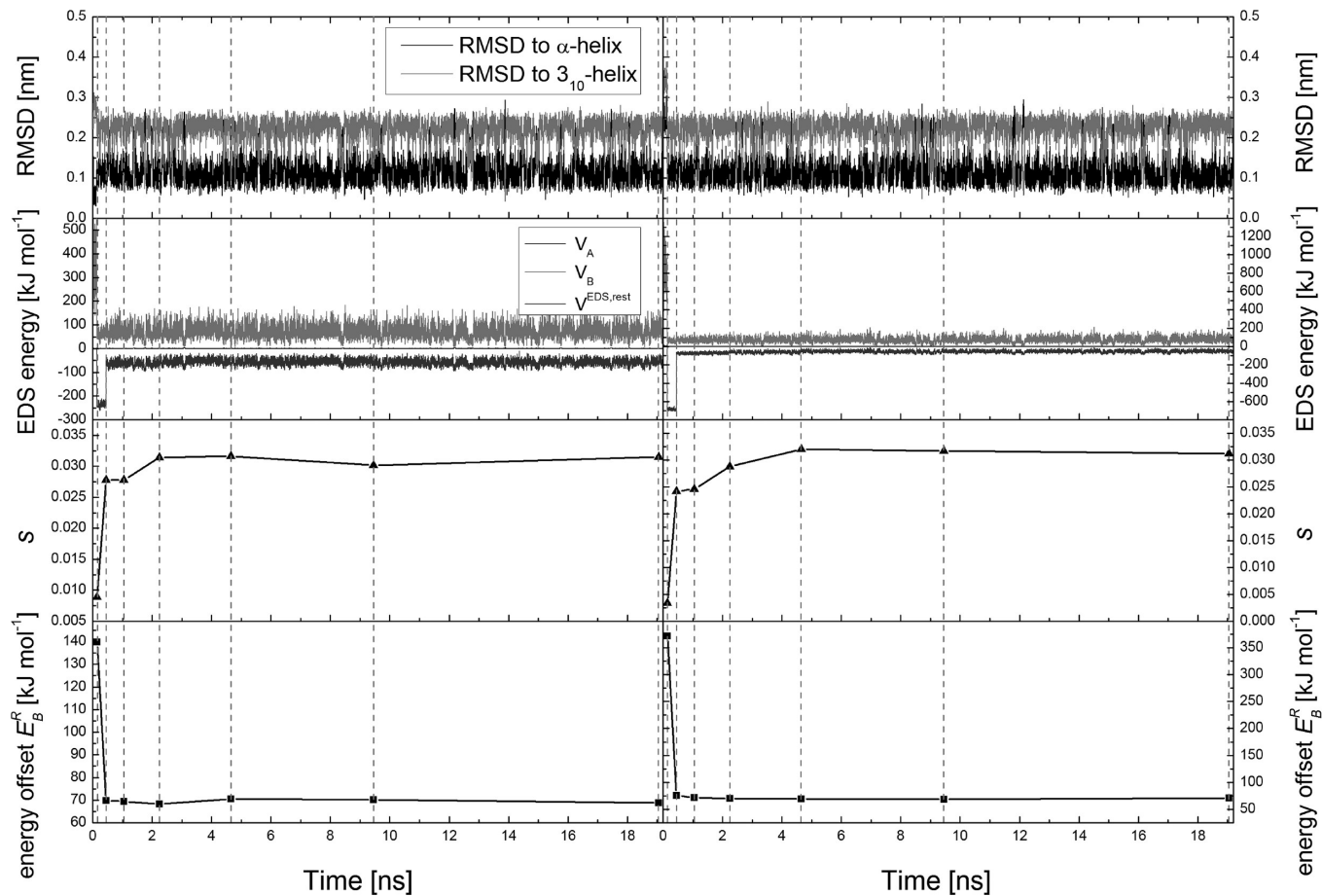


Figure 9. Time evolutions of different properties in the α -helix/3₁₀-helix EDS parameter update simulations *update7* (left panels) and *update8* (right panels), see also Table 1. From top to bottom: backbone atom-positional RMSD of the peptide with respect to the α -helix or 3₁₀-helix, the restraining and the EDS reference potential energies, smoothness parameter *s*, energy offset E_B^R . The vertical dashed lines show when the updates of *s* and E_B^R are carried out.

reasonable range. Moreover, there may be more than one set of EDS parameters that allows optimal sampling of both end states *A* and *B* using the reference-state Hamiltonian H_R . Trying yet other update schemes would not help to converge the parameters, because the limiting factor is the relatively long residence time required at the end states. Longer time periods between updates or the use of enhanced sampling techniques may improve the convergence of the *s* and E_B^R parameters.

Time evolutions of backbone atom-positional RMSD of the peptide, of ΔG_{BA} and $\Delta G_{\pi\alpha}$ in the four EDS evaluation simulations (Table 1) are shown in Figure 8. ΔG_{BA} was calculated through eq 20 and does not depend explicitly on the number of configurations belonging to each of the conformational sets α and β , whereas $\Delta G_{\pi\alpha}$ was calculated through eq 22 and does depend on them. Nevertheless, the two properties show a similar trend in all four simulations; i.e., the free enthalpy differences tend to increase when set α is sampled and to decrease when set β is sampled. Though having quite different *s* and E_B^R parameters, the four EDS simulations gave similar pictures, except for the relative populations of the two conformational sets α and β . The curves of ΔG_{BA} become flat after 20–30 ns (Figures 8 and S4, Supporting Information), while the convergence of $\Delta G_{\pi\alpha}$ is slower because the relative population of the conformational set β versus set α (the last term in eq 22) converges slower, i.e., after 20–40 ns

(Figures 8 and S5, Supporting Information). Again, application of enhanced sampling techniques might speed up the convergence of the free enthalpy differences.

The results for ΔG_{BA} and $\Delta G_{\pi\alpha}$ in the four EDS evaluation simulations are shown in Table 2. The difference in ΔG_{BA} among the four simulations is about 3 kJ mol⁻¹. The block averaging used underestimates, with values less than 1 kJ mol⁻¹, the statistical uncertainties of the results. For $\Delta G_{\pi\alpha}$, the difference among the four values is within 1 kJ mol⁻¹. The EDS results for both free enthalpy differences are consistent with the corresponding ones obtained from the TI and end-state simulations.

The results of the EDS calculations to obtain the free enthalpy difference $\Delta G_{310\alpha}$ between a 3₁₀-helix and an α -helix for deca-alanine in aqueous solution are shown in Figures 9 and 10. Various quantities for two EDS parameter update simulations connecting two end states *A* (α -helix) and *C* (3₁₀-helix), *update7* and *update8*, are shown in Figure 9. The convergence of the *s* and E_B^R parameters is much faster than for the EDS simulations connecting the end states *A* (α -helix) and *B* (π -helix), probably due to a larger overlap of the phase spaces between the end states *A* and *C*. The resulting *s* and E_B^R parameters are 0.03 and 68.7 kJ mol⁻¹ and 0.03 and 70.5 kJ mol⁻¹ for the *update7* and *update8* simulations, respectively. The RMSD, ΔG_{CA} , and $\Delta G_{310\alpha}$ for the EDS evaluation simulation, EDS7, are shown in Figure 10. Although E_B^R is very big and many transition events were

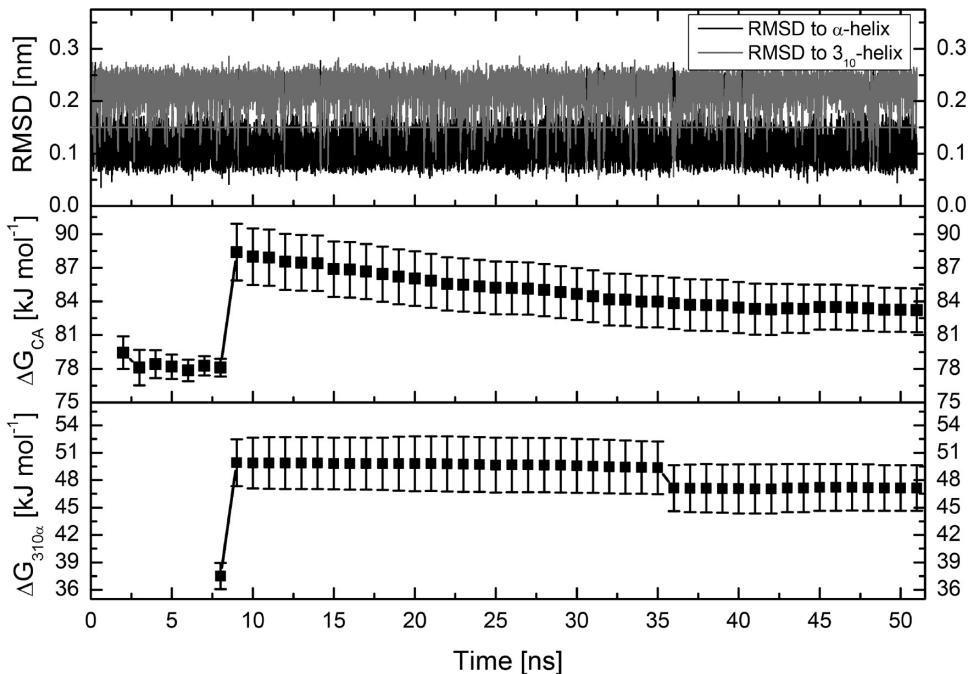


Figure 10. Time evolutions of backbone atom-positional RMSD of the peptide with respect to the α -helix or 3_{10} -helix, free enthalpy differences of the two end-state Hamiltonians C (3_{10} -helix) and A (α -helix), ΔG_{CA} , and free enthalpy differences of the two conformational sets β (3_{10} -helix) and α (α -helix), $\Delta G_{310\alpha}$ in EDS evaluation simulation EDS7.

occurring, the simulation sampled mostly the α -helix. The results are 83.2 ± 1.9 kJ mol⁻¹ and 47.1 ± 2.5 kJ mol⁻¹ for ΔG_{CA} and $\Delta G_{310\alpha}$, respectively.

4.4. Free Enthalpy Differences between Three Helices. According to the EDS simulations, the free enthalpy differences of the π -helix and the 3_{10} -helix versus the α -helix are 5 kJ mol⁻¹ and 47 kJ mol⁻¹, respectively, for the alanine deca-peptide using the GROMOS 53A6 force field in SPC water solvent. That is, the α -helix and the π -helix are of similar stability, whereas the 3_{10} -helix is very unstable for deca-alanine. In a different context, studies²¹ have shown that for the CHARMM 22 force field, these values are -1.9 kcal mol⁻¹ and 20.9 kcal mol⁻¹ for the free enthalpy differences of the π -helix and the 3_{10} -helix versus the α -helix of deca-alanine in TIP3P water solvent. Unfortunately, no corresponding experimental data are available for deca-alanine in aqueous solution.

5. CONCLUSION

In this work, statistical-mechanical expressions were formulated which allow the application of the technique of enveloping distribution sampling (EDS) to the computation of free enthalpy differences between different conformations or conformational states instead of between different Hamiltonians. Different helical conformations, i.e., 3_{10} , α -, and π -helices, of an alanine deca-peptide in explicit water solvent were considered. The results were compared to those obtained from the standard technique of thermodynamic integration (TI) and from end-state simulations.

A reasonably accurate result was obtained using TI simulations, in which the λ -dependent pathway was defined on the basis of the hydrogen bonds characterizing the different helical conformations. Because this pathway involves an energetic barrier in the physical potential energy V^{phys} , a large change occurred in the

$\langle (\partial V_{\text{TI}})/(\partial \lambda) \rangle_\lambda$ curve for λ values at the barrier. Moreover, it is difficult to converge $\langle (\partial V_{\text{TI}})/(\partial \lambda) \rangle_\lambda$ in the simulations at intermediate λ values due to the instability of the conformations near the barrier. Thus, the TI result suffers from statistical uncertainty. One may argue that TI might have produced a better result if a better pathway, i.e., λ -dependence of the biasing potential energy terms, had been defined. However, often a “better” pathway that avoids a barrier is not so easily found. This is one of the drawbacks of the TI method.

This situation can be avoided by estimating the free enthalpy difference based on end-state simulations. However, in that case, overlap of conformational space between the two end states is required for such calculations to yield meaningful results.

In the two-state EDS simulations, an unphysical reference-state Hamiltonian which allows sampling of the conformations relevant to the different end states is constructed automatically. Both helices were sampled during the simulations, and the transitions between them were on the time scale of nanoseconds, which makes the convergence of the EDS smoothness parameter and the EDS energy offset parameter to their “optimal” values slow. However, the resulting EDS parameters of the different EDS parameter update simulations were in a reasonable range. Extending the time period between updates did speed up the convergence, whereas the exclusion of conformations not relevant to the two conformations did not improve the convergence in this case.

The EDS evaluation simulations using these EDS reference states were used to calculate the free enthalpy differences between the two end states and between the two helical conformations. The different EDS reference-state Hamiltonians gave similar results. According to the EDS simulations, for the deca-alanine using the GROMOS 53A6 force field and SPC water as the solvent, the α -helix and the π -helix are of similarly stability, whereas the 3_{10} -helix is very unstable.

The presented EDS method can be considered as a particular type of umbrella sampling, with an automatically generated biasing umbrella potential energy function of the particular form eq 2, which is solely based on end-state potential energy functions and which ensures the sampling of both end-state conformations. We have shown that the EDS method is applicable to computing conformational free energy differences as well as alchemical ones. Only two-state problems were considered, but the method can be generalized to multiple-state problems and can be further optimized by combination with techniques to speed up the sampling of conformational space.

■ APPENDIX

Equation 22 can be derived as follows. According to eq 21, we have

$$\begin{aligned} \Delta G_{\beta\alpha} &= G_\beta - G_\alpha \\ &= -k_B T \ln \left\{ \frac{\int e^{-V^{\text{phys}}(\vec{r}^N)/k_B T} \delta(\vec{r}^N - \vec{r}_\beta^N) d\vec{r}^N}{\int e^{-V^{\text{phys}}(\vec{r}^N)/k_B T} \delta(\vec{r}^N - \vec{r}_\alpha^N) d\vec{r}^N} \right\} \end{aligned} \quad (31)$$

where $\delta(\vec{r}^N - \vec{r}_\xi^N)$ is the delta function that selects configurations that belong to set ξ . Using eq 2, we can rewrite eq 31 as

$$\begin{aligned} \Delta G_{\beta\alpha} &= -k_B T \\ &\times \ln \left\{ \frac{\int e^{+V^{\text{EDS,rest}}(\vec{r}^N)/k_B T} \times e^{-V_R(\vec{r}^N)/k_B T} \times \delta(\vec{r}^N - \vec{r}_\beta^N) d\vec{r}^N}{\int e^{-V_R(\vec{r}^N)/k_B T} \times \delta(\vec{r}^N - \vec{r}_\beta^N) d\vec{r}^N} \right. \\ &\times \frac{\int \delta(\vec{r}^N - \vec{r}_\beta^N) \times e^{-V_R(\vec{r}^N)/k_B T} d\vec{r}^N}{\int e^{-V_R(\vec{r}^N)/k_B T} d\vec{r}^N} \\ &\times \frac{\int e^{-V_R(\vec{r}^N)/k_B T} d\vec{r}^N}{\int \delta(\vec{r}^N - \vec{r}_\alpha^N) \times e^{-V_R(\vec{r}^N)/k_B T} d\vec{r}^N} \\ &\times \frac{\int \delta(\vec{r}^N - \vec{r}_\alpha^N) \times e^{-V_R(\vec{r}^N)/k_B T} d\vec{r}^N}{\int e^{+V^{\text{EDS,rest}}(\vec{r}^N)/k_B T} \times e^{-V_R(\vec{r}^N)/k_B T} \times \delta(\vec{r}^N - \vec{r}_\alpha^N) d\vec{r}^N} \\ &= -k_B T \ln \left\{ \frac{\langle e^{+V^{\text{EDS,rest}}/k_B T} \rangle_{R,\text{set}\beta}}{\langle e^{+V^{\text{EDS,rest}}/k_B T} \rangle_{R,\text{set}\alpha}} \times \frac{\langle \delta(\vec{r}^N - \vec{r}_\beta^N) \rangle_R}{\langle \delta(\vec{r}^N - \vec{r}_\alpha^N) \rangle_R} \right\} \end{aligned} \quad (32)$$

Using eq 23 in eq 32, we find eq 22.

Using the definition $V_X = V_X^{\text{phys}} + V_X^{\text{rest}}$ for $X = A$ and $X = B$, eq 31 can also be rewritten as

$$\begin{aligned} \Delta G_{\beta\alpha} &= -k_B T \\ &\times \ln \left\{ \frac{\int e^{+V_B^{\text{rest}}(\vec{r}^N)/k_B T} \times e^{-V_B(\vec{r}^N)/k_B T} \times \delta(\vec{r}^N - \vec{r}_\beta^N) d\vec{r}^N}{\int e^{-V_B(\vec{r}^N)/k_B T} \times \delta(\vec{r}^N - \vec{r}_\beta^N) d\vec{r}^N} \right. \\ &\times \frac{\int \delta(\vec{r}^N - \vec{r}_\beta^N) \times e^{-V_B(\vec{r}^N)/k_B T} d\vec{r}^N}{\int e^{-V_B(\vec{r}^N)/k_B T} d\vec{r}^N} \end{aligned}$$

$$\begin{aligned} &\times \frac{\int e^{-V_B(\vec{r}^N)/k_B T} d\vec{r}^N}{\int e^{-(V_M(\vec{r}^N) - V_B(\vec{r}^N))/k_B T} \times e^{-V_B(\vec{r}^N)/k_B T} d\vec{r}^N} \\ &\times \frac{\int e^{-(V_M(\vec{r}^N) - V_A(\vec{r}^N))/k_B T} \times e^{-V_A(\vec{r}^N)/k_B T} d\vec{r}^N}{\int e^{-V_A(\vec{r}^N)/k_B T} d\vec{r}^N} \\ &\times \frac{\int e^{-V_A(\vec{r}^N)/k_B T} d\vec{r}^N}{\int \delta(\vec{r}^N - \vec{r}_\alpha^N) \times e^{-V_A(\vec{r}^N)/k_B T} d\vec{r}^N} \\ &\times \frac{\int e^{-V_A(\vec{r}^N)/k_B T} \times \delta(\vec{r}^N - \vec{r}_\alpha^N) d\vec{r}^N}{\int e^{+V_A^{\text{rest}}(\vec{r}^N)/k_B T} \times e^{-V_A(\vec{r}^N)/k_B T} \times \delta(\vec{r}^N - \vec{r}_\alpha^N) d\vec{r}^N} \Big\} \\ &= -k_B T \ln \left\{ \frac{\langle e^{+V_B^{\text{rest}}/k_B T} \rangle_{B,\text{set}\beta}}{\langle e^{+V_A^{\text{rest}}/k_B T} \rangle_{A,\text{set}\alpha}} \times \frac{\langle 1 \rangle_{B,\text{set}\beta}}{\langle 1 \rangle_{A,\text{set}\alpha}} \times \frac{\langle e^{-(V_M - V_A)/k_B T} \rangle_A}{\langle e^{-(V_M - V_B)/k_B T} \rangle_B} \right\} \end{aligned} \quad (33)$$

which is eq 25.

■ ASSOCIATED CONTENT

S Supporting Information. The RMSD curves and the hydrogen-bond populations of the end-state simulations are available. This information is available free of charge via the Internet at <http://pubs.acs.org/>.

■ AUTHOR INFORMATION

Corresponding Author

*E-mail: wfvgn@igc.phys.chem.ethz.ch.

■ ACKNOWLEDGMENT

This work was financially supported by the National Center of Competence in Research (NCCR) in Structural Biology and by grant number 200020-121913 of the Swiss National Science Foundation, by grant number 228076 of the European Research Council (ERC), and by grants numbers IZLCZ2-123884 (Swiss) and GJHZ0906 (Chinese) of the Sino–Swiss Science and Technology Cooperation Program, which is gratefully acknowledged.

■ REFERENCES

- (1) Straatsma, T. P.; McCammon, J. A. *Annu. Rev. Phys. Chem.* **1992**, 43, 407–435.
- (2) Kollman, P. *Chem. Rev.* **1993**, 93, 2395–2417.
- (3) Simonson, T.; Archontis, G.; Karplus, M. *Acc. Chem. Res.* **2002**, 35, 430–437.
- (4) van Gunsteren, W. F.; Daura, X.; Mark, A. E. *Helv. Chim. Acta* **2002**, 85, 3113–3129.
- (5) Kofke, D. A. *Fluid Phase Equilib.* **2005**, 228, 41–48.
- (6) Rodinger, T.; Pomes, R. *Curr. Opin. Struct. Biol.* **2005**, 15, 164–170.
- (7) Gilson, M. K.; Zhou, H. X. *Annu. Rev. Biophys. Biomol. Struct.* **2007**, 36, 21–42.
- (8) Meirovitch, H. *Curr. Opin. Struct. Biol.* **2007**, 17, 181–186.
- (9) Jorgensen, W. L.; Thomas, L. L. *J. Chem. Theory Comput.* **2008**, 4, 869–876.
- (10) Knight, J. L.; Brooks, C. L. *J. Comput. Chem.* **2009**, 30, 1692–1700.

- (11) Vanden-Eijnden, E. *J. Comput. Chem.* **2009**, *30*, 1737–1747.
- (12) Christ, C. D.; Mark, A. E.; van Gunsteren, W. F. *J. Comput. Chem.* **2010**, *31*, 1569–1582.
- (13) Postma, J. P. M.; Berendsen, H. J. C.; Haak, J. R. *Faraday Symp. Chem. Soc.* **1982**, *17*, 55–67.
- (14) Grossfield, A.; Ren, P. Y.; Ponder, J. W. *J. Am. Chem. Soc.* **2003**, *125*, 15671–15682.
- (15) Jorgensen, W. L. *Science* **2004**, *303*, 1813–1818.
- (16) Oostenbrink, C.; van Gunsteren, W. F. *Proc. Natl. Acad. Sci. U.S.A.* **2005**, *102*, 6750–6754.
- (17) Daura, X.; Jaun, B.; Seebach, D.; van Gunsteren, W. F.; Mark, A. E. *J. Mol. Biol.* **1998**, *280*, 925–932.
- (18) Brooks, C. L. *Acc. Chem. Res.* **2002**, *35*, 447–454.
- (19) Roux, B.; Karplus, M. *Biophys. J.* **1991**, *59*, 961–981.
- (20) Hansen, H. S.; Hunenberger, P. H. *J. Chem. Theory Comput.* **2010**, *6*, 2622–2646.
- (21) Mahadevan, J.; Lee, K. H.; Kuczera, K. *J. Phys. Chem. B* **2001**, *105*, 1863–1876.
- (22) Wang, J.; Gu, Y.; Liu, H. Y. *J. Chem. Phys.* **2006**, *125*, 094907.
- (23) Torrie, G. M.; Valleau, J. P. *J. Comput. Phys.* **1977**, *23*, 187–199.
- (24) Hansen, H. S.; Hunenberger, P. H. *J. Comput. Chem.* **2010**, *31*, 1–23.
- (25) Kirkwood, J. G. *J. Chem. Phys.* **1935**, *3*, 300–313.
- (26) Zwanzig, R. W. *J. Chem. Phys.* **1954**, *22*, 1420–1426.
- (27) Powles, J. G.; Evans, W. A. B.; Quirke, N. *Mol. Phys.* **1982**, *46*, 1347–1370.
- (28) Shing, K. S.; Gubbins, K. E. *Mol. Phys.* **1982**, *46*, 1109–1128.
- (29) Bennett, C. H. *J. Comput. Phys.* **1976**, *22*, 245–268.
- (30) Konig, G.; Bruckner, S.; Boresch, S. *J. Comput. Chem.* **2009**, *30*, 1712–1718.
- (31) Lu, N. D.; Kofke, D. A.; Woolf, T. B. *J. Comput. Chem.* **2004**, *25*, 28–39.
- (32) Lu, N. D.; Singh, J. K.; Kofke, D. A. *J. Chem. Phys.* **2003**, *118*, 2977–2984.
- (33) Liu, H. Y.; Mark, A. E.; van Gunsteren, W. F. *J. Phys. Chem.* **1996**, *100*, 9485–9494.
- (34) Christ, C. D.; van Gunsteren, W. F. *J. Chem. Phys.* **2007**, *126*, 184110.
- (35) Christ, C. D.; van Gunsteren, W. F. *J. Chem. Phys.* **2008**, *128*, 174112.
- (36) Christ, C. D.; van Gunsteren, W. F. *J. Chem. Theory Comput.* **2009**, *5*, 276–286.
- (37) Christ, C. D.; van Gunsteren, W. F. *J. Comput. Chem.* **2009**, *30*, 1664–1679.
- (38) Riniker, S.; Christ, C. D.; Hansen, N.; Mark, A. E.; Nair, P. C.; van Gunsteren, W. F. *J. Chem. Phys.* **2011**, *135*, 024105.
- (39) Hansen, N.; Dolenc, J.; Knecht, M.; Riniker, S.; van Gunsteren, W. F. *J. Comput. Chem.* **2011**, accepted.
- (40) Lin, Z. X.; Kornfeld, J.; Machler, M.; van Gunsteren, W. F. *J. Am. Chem. Soc.* **2010**, *132*, 7276–7278.
- (41) Oostenbrink, C.; Villa, A.; Mark, A. E.; van Gunsteren, W. F. *J. Comput. Chem.* **2004**, *25*, 1656–1676.
- (42) Berendsen, H. J. C.; Postma, J. P. M.; van Gunsteren, W. F.; Hermans, J. In *Intermolecular forces*; Pullman, B., Ed.; Reidel: Dordrecht, The Netherlands, 1981; pp 331–342.
- (43) van Gunsteren, W. F.; Billeter, S. R.; Eising, A. A.; Hünenberger, P. H.; Krüger, P.; Mark, A. E.; Scott, W. R. P.; Tironi, I. G. *Biomolecular Simulation: The GROMOS96 Manual and User Guide*; Vdf Hochschulverlag AG an der ETH Zürich: Zürich, Switzerland, 1996.
- (44) Christen, M.; Hünenberger, P. H.; Bakowies, D.; Baron, R.; Bürgi, R.; Geerke, D. P.; Heinz, T. N.; Kastenholz, M. A.; Kräutler, V.; Oostenbrink, C.; Peter, C.; Trzesniak, D.; van Gunsteren, W. F. *J. Comput. Chem.* **2005**, *26*, 1719–1751.
- (45) Riniker, S.; Christ, C. D.; Hansen, H. S.; Hünenberger, P. H.; Oostenbrink, C.; Steiner, D.; van Gunsteren, W. F. *J. Phys. Chem. B* **2011**; DOI: 10.1021/jp204303a.
- (46) Berendsen, H. J. C.; Postma, J. P. M.; van Gunsteren, W. F.; DiNola, A.; Haak, J. R. *J. Chem. Phys.* **1984**, *81*, 3684–3690.
- (47) Ryckaert, J. P.; Ciccotti, G.; Berendsen, H. J. C. *J. Comput. Phys.* **1977**, *23*, 327–341.
- (48) Tironi, I. G.; Sperb, R.; Smith, P. E.; van Gunsteren, W. F. *J. Chem. Phys.* **1995**, *102*, 5451–5459.
- (49) Allen, M. P.; Tildesley, D. J. *Computer Simulation of Liquids*; Oxford University Press: New York, 1987; pp 191–195.